

**Technical Report on the Development of a
Microwave Engine for Satellite Propulsion**

Roger J. Shawyer

July 2006 Issue 2

Prepared for
Research and Development Project Ref. 1939
SEEDA
Department of Trade and Industry

©Satellite Propulsion Research Ltd 2006
Tel 44 (0) 1243 377783
Email: rjshawyer@aol.com

The copyright in this document is the property of Satellite Propulsion Research Ltd.
The document contains PROPRIETARY INFORMATION which must not be
disclosed without prior approval

CONTENTS

1. Introduction
2. Description of engine
 - 2.1. Principles of operation
 - 2.2. Engine system
 - 2.3. Thruster design
 - 2.4. Feed assembly
 - 2.5. Magnetron and power supply
 - 2.6. Thermal subsystem
 - 2.7. Telemetry and command subsystem
3. Engine test programme
 - 3.1. Small signal tests
 - 3.2. High power tests
 - 3.3. Vertical thrust tests
 - 3.3.1. Description of test rig
 - 3.3.2. Test results
 - 3.4. Horizontal thrust tests
 - 3.4.1. Description of test rig
 - 3.4.2. Test results
4. Summary and conclusions
5. Further Work

1. INTRODUCTION

This report documents the work that was carried out to design, build and test a Demonstrator Engine based on a radical new concept of microwave propulsion for spacecraft. The work is a continuation of the experimental microwave thruster project described in REF 1 which was supported by the Department of Trade and Industry under the SMART Feasibility Study Ref 931.

This present work was again supported by the Department of Trade and Industry under a Research and Development Grant.

REF 1. Technical Report on the Experimental Microwave Thruster.

Roger J. Shawyer

September 2002 Issue 2

2.DESCRPTION OF ENGINE

2.1.Principles of Operation

The following section gives a simplified, illustrative description of the principles of operation, based on the standard text book interpretation of the propagation mechanism for an Electromagnetic wave within a waveguide. For a full mathematical approach to the principles of operation, see REF 2.

2.1.1. Free Space Propagation

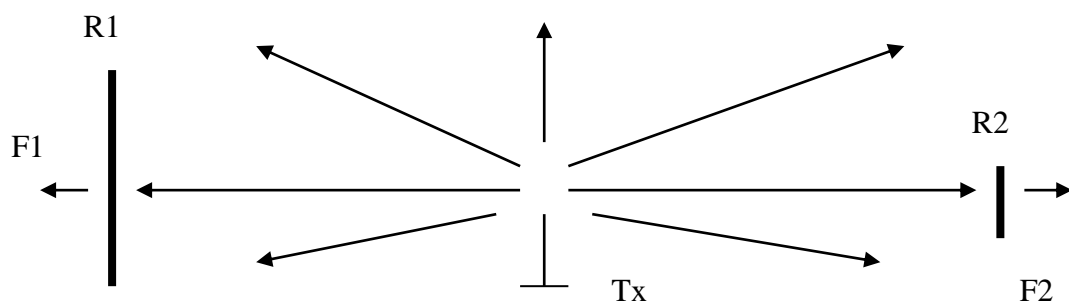


Fig 2.1.1

Assume two reflective plates R1 and R2 are placed equidistance from a transmitter Tx in free space. The area of R1 is greater than R2, therefore the power incident on R1 is greater than R2, and therefore the force F1 is greater than F2. If the two plates are connected together the resultant force $F1-F2$ will cause the assembly to move a distance m in accordance with Newtons laws.

If m is small compared to the distance between the plates the movement of the assembly will have no effect on reflected powers or forces. In a similar manner, movement of the transmitter by distance m will have no effect.

This independence of transmitter and plate movement, leads to the conclusion that if the transmitter and the plates are connected, the whole assembly will move. Whatever the final speed of movement achieved, the propagation velocity remains c , the velocity of light in free space.

2.1.2. Propagation in a wide waveguide

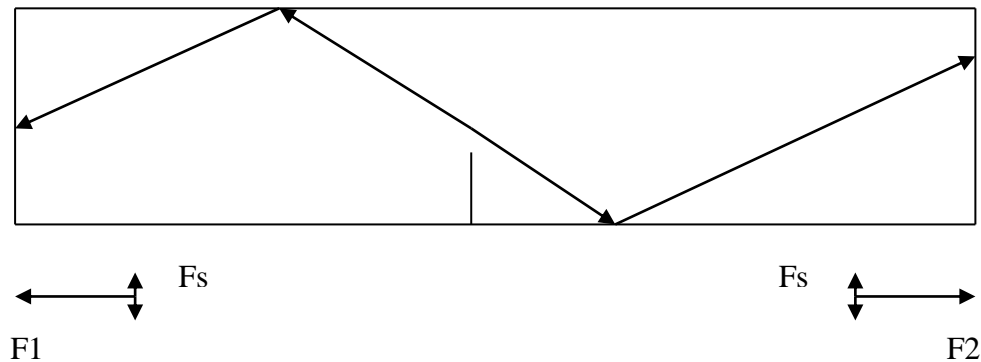


Fig 2.1.2

Assume the two reflective plates, now the same size, form the end plates of a wide waveguide. The propagation path is constrained by reflection from the side walls of the waveguide and forms a sawtooth pattern as shown. The velocity of the microwave energy in the axial direction, termed the group velocity, is now below the value of c due to the longer, sawtooth path travelled by the wave.

Resolution of the forces at the two ends of the waveguide give equal opposing forces F_1 and F_2 and small orthogonal side wall forces F_s .

2.1.3. Propagation in a narrow waveguide

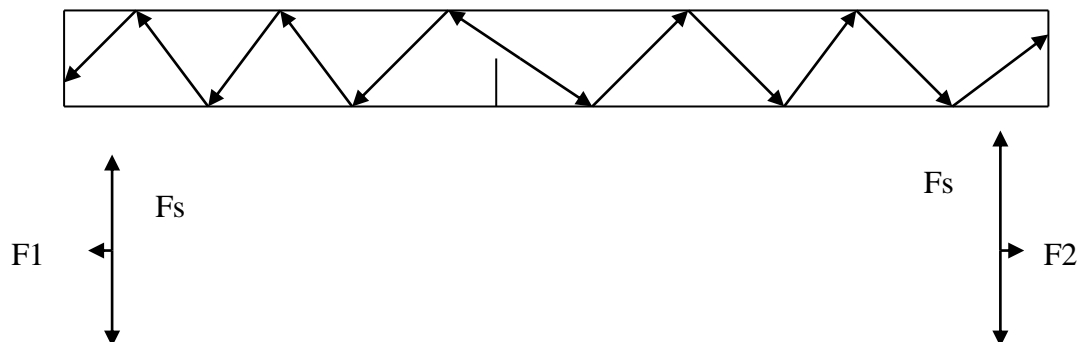


Fig 2.1.3

Assume the waveguide is now narrow compared to 2.1.2. with the result that the sawtooth becomes sharper. In this case the group velocity in the axial direction along the waveguide becomes an even small fraction of c , as the sawtooth path the wave must travel is longer than in 2.1.2.

Resolution of the forces now gives a smaller value of F_1 and F_2 , due to the lower axial velocity at which the energy is being reflected. However a much higher value of sidewall force F_s is experienced.

2.1.4 Propagation in a tapered waveguide

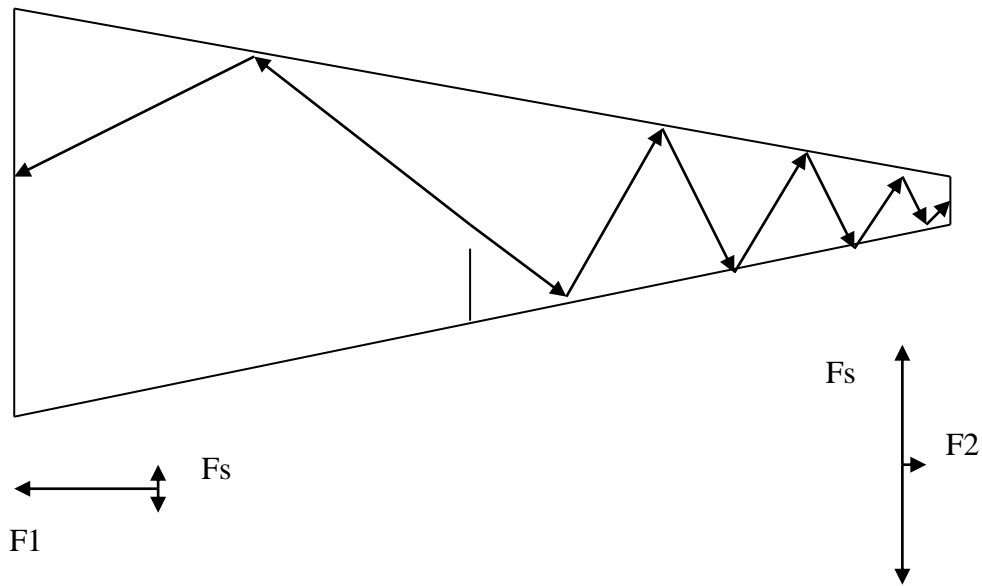


Fig 2.1.4

Assume that the waveguide is now tapered as shown. In this case the group velocity is higher at the wide end than at the narrow end. Thus resolution of the forces shows F_1 is greater than F_2 , whereas the sidewall force F_s is higher at the narrow end than the wide end.

As with the free space example in 2.1.1, the force difference $F_1 - F_2$ will give rise to movement of the waveguide, but this will have no effect on the propagation velocities within the waveguide.

2.1.5 Propagation in a resonant tapered waveguide

As with any microwave cavity, if the axial path length is a multiple of half the mean guide wavelength, at the frequency of operation, then the waveguide will form a resonant cavity. The electrical and magnetic fields at each end plate will add in phase, to give instantaneous powers equal to Q times the transmitted power. This will give rise to a force difference equal to $Q(F_1 - F_2)$. Note that in a well designed cavity the unloaded Q can reach values greater than 50,000. It is this high multiplication of the small force difference that gives the engine a useful net force.

REF 2. A Theory of Microwave Propulsion for Spacecraft.

Roger J. Shawyer

SPR Ltd V.9.3 2006

2.2 Engine System

The engine system design work was preceded by a short mission analysis phase to ensure that the resulting design was compatible with the highest number of near term missions. The power rating of the Demonstrator engine was decided by reviewing the mass and power specifications of the latest communication satellites and their launch, attitude-control and orbit-maintenance requirements. For example, taking HOTBIRD 8 as typical, with a mass of 5 tonnes and a power of 14 kW, a configuration of 4 engines would be proposed. Each engine, nominally 3.5 kW, would have two operating magnetrons in a 2 for 3 redundancy configuration. For 70% efficiency, each magnetron would supply 1.2 kW of microwave power. The Demonstrator engine therefore has one magnetron of 1.2 kW maximum power, as a demonstration of principle.

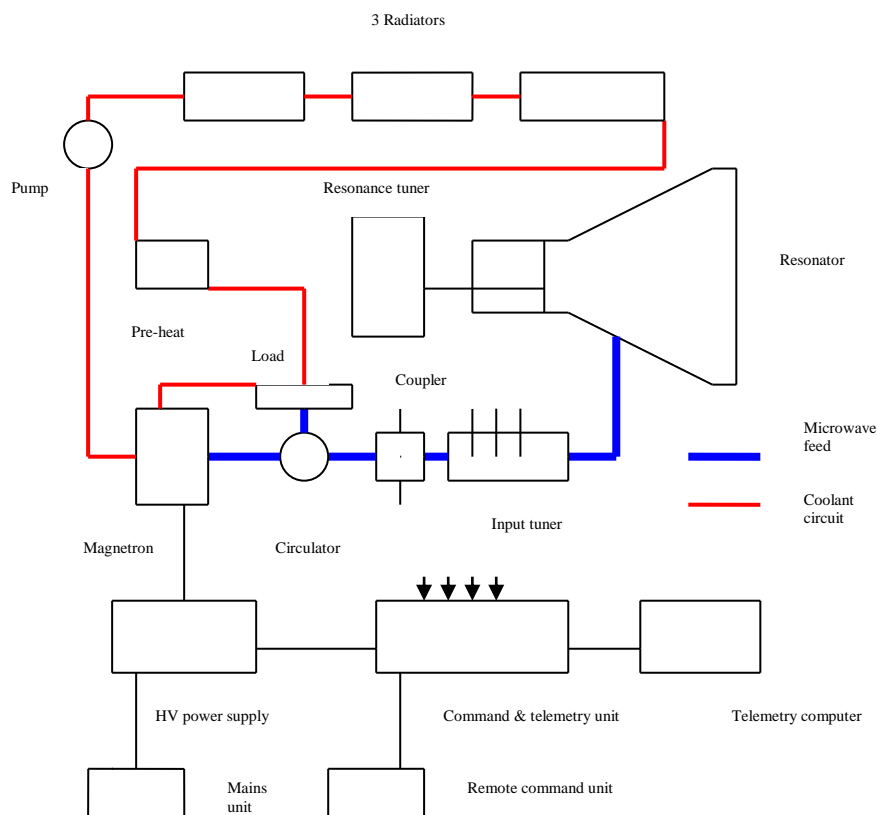


Fig 2.2.1

Fig 2.2.1 gives a simplified schematic diagram of the engine and its supporting units. The basic thruster consists of a resonator and a resonance tuner. The thruster is fed microwave power from the magnetron via a feed assembly comprising a circulator and load, (which together form an isolator), a dual coupler and an input tuner. The magnetron and load are cooled by a pumped coolant circuit containing three radiators and a preheat unit.

The magnetron, feed assembly and thruster are mounted in an open steel thrust frame, which provides attachment to test rigs in five thrust configurations. These give the following thrust vector directions:

Vertical up
Vertical down
Horizontal forward
Horizontal reverse
Horizontal axial

The thermal subsystem, complete with telemetry and power interfaces, is mounted in an open aluminium U frame, which fits over and is attached to the thrust frame.

The magnetron is powered from a High Voltage Power Supply Unit (HVPSU) and the engine is controlled and monitored by a Telemetry and Command Unit (TCU). This unit, together with the HVPSU and a laptop Telemetry Computer is mounted separately on an instrumentation platform on the test rig.

A Mains Power Unit and Remote Command Unit are mounted off the test rig. Fig 2.2.2. shows the complete engine.

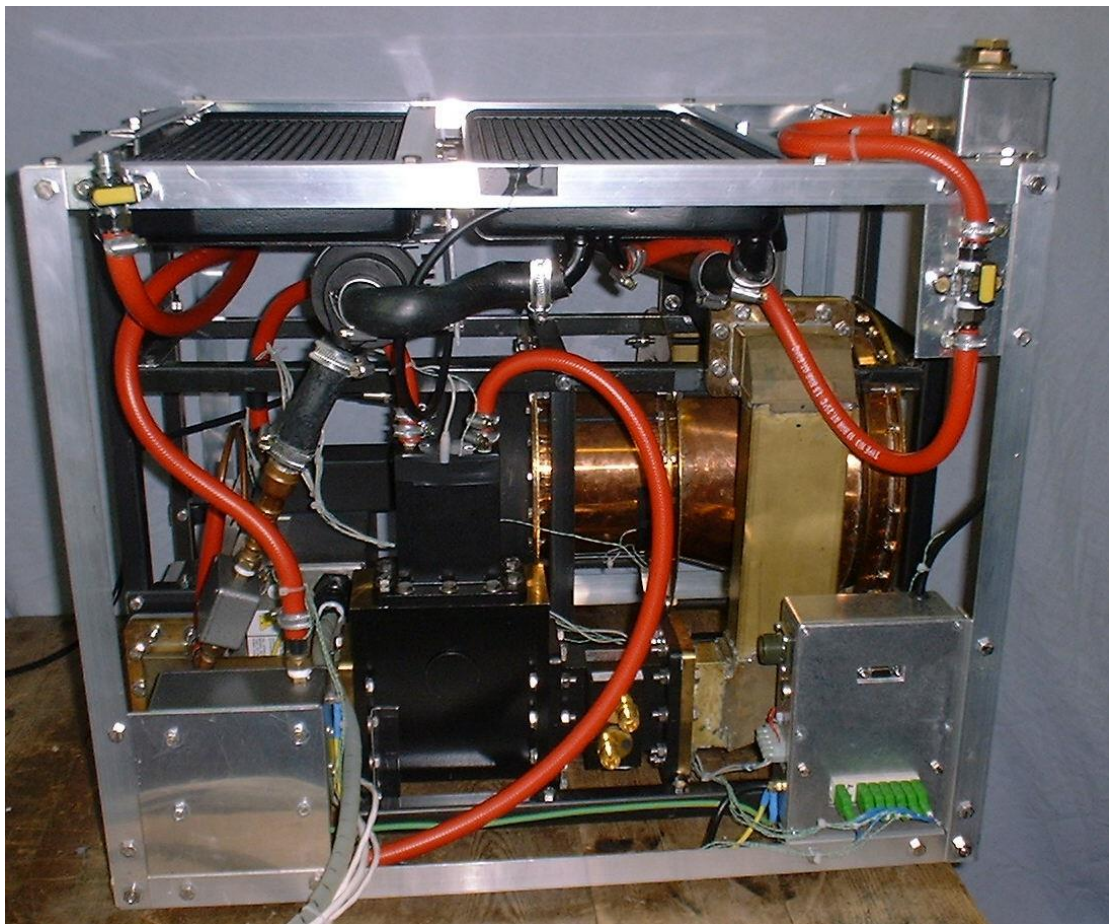


Fig 2.2.2

2.3 Thruster Design

The software developed during the design of the experimental thruster was updated and used in an iterative design process to optimise the geometry of the resonator and tuning sections of the Demonstrator engine. The resulting design (at the seventh iteration) was the basis for further detail consideration of the thermal stability and tuning resolution requirements. A review of the potential for resonance in spurious modes was carried out, by running the software for twelve different modes, from TE01 to TE22 and TM01 to TM22.

The design resulted in a maximum diameter of 280 mm operating at 2450 MHz, with a Design Factor of 0.844. This can be compared to the earlier experimental thruster with a maximum diameter of 160 mm and a Design Factor of .497, at the same operating frequency.

A signal level analysis was carried out for the resonator coupled to the feed and instrumentation components, to allow specifications for these items to be prepared. To support the microwave design work, a low power test bench was set up. This was calibrated against the experimental thruster, and then used to verify the microwave design of the Demonstrator engine.

The design of the tuning section incorporates a stepper motor, gear train and lead screw, together with the necessary electronics to give the very high resolution tuning required by the Q value of 72,000 that is theoretically obtainable with the resonator.

The mechanical design was based on a fabricated copper resonator and tuner supported by brass plates held together with a combination of brass and invar tie rods. This construction, together with a steel lead screw allows the different expansion coefficients of the four materials to be used to provide inherent thermal compensation. This was considered essential to maintain a stable resonance frequency over the required temperature range.

Thermal design software was developed to enable optimisation of the dimensions to obtain full thermal compensation over a 35 degree temperature range.

The thruster is illustrated in fig 2.3.1

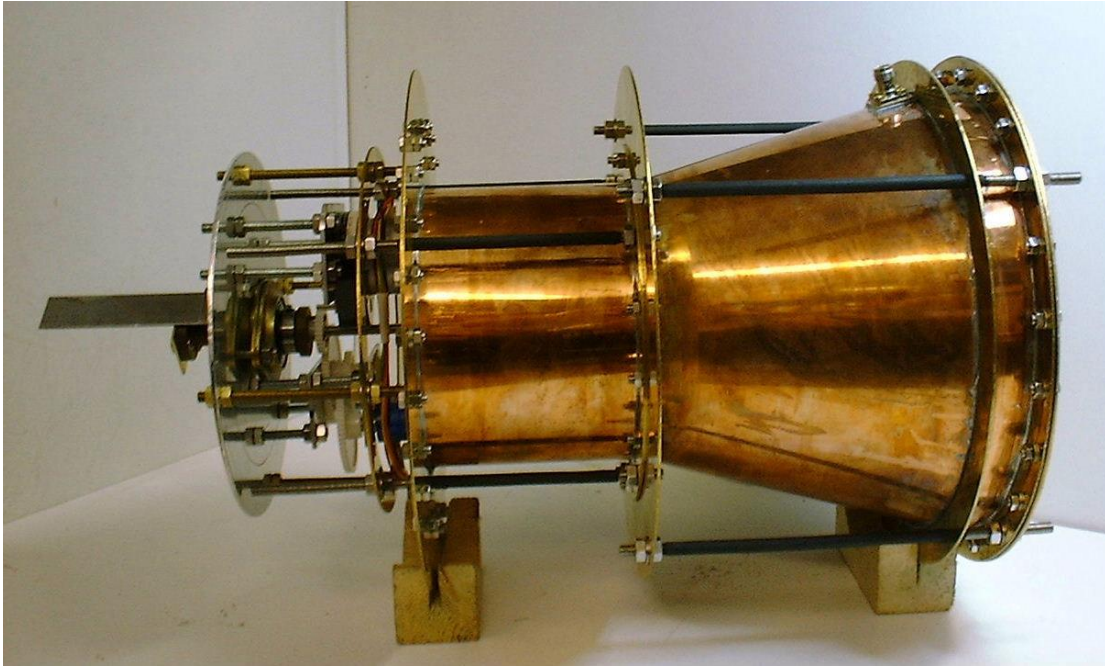


Fig 2.3.1

2.4 Feed Assembly

The WR284 waveguide output of the magnetron is connected through a 90deg E bend assembly to an isolator. The isolator consists of a circulator and load. The circulator, type WR284CIRC3A, is rated at 3kW with a 0.2dB insertion loss. The water cooled load, type GA1201, is also rated at 3kW, with a minimum return loss of 23dB. The load is specified up to maximum input water temperature of 50 deg C.

Power is then fed through a dual coupler, type GA3102, to monitor forward and reflected power. The coupling factor is 56dB, with a minimum specified directivity of 25dB.

The feed from the coupler is via a waveguide assembly containing both a 90 deg H bend and a 90 deg E bend, to reach the input tuner, situated above the large diameter end of the resonator. This position enables easy access to the stub adjusters. The GA1001 precision 3 stub tuner has stubs spaced at $\frac{1}{4}$ wavelength intervals, offset $\frac{1}{16}$ guide wavelength from centre. The stub housings are designed with reactive chokes for high Q applications.

Power is finally fed to the resonator input via a U shaped waveguide assembly, containing two 90 deg E bends. All waveguide is standard WR284 (WG10) brass, with type CPR 284F brass flanges. Although the resulting feed assembly is heavy compared to flight waveguide, it is rugged and easily fabricated.

2.5 Magnetron and Power Supply

The magnetron and power supply were procured as a complete microwave generator set, type GA4305 from a US supplier. The set consisted of a separate magnetron head unit and a switched mode power supply, with an interconnecting cable harness.

The magnetron itself is a water-cooled, 2M137 device, rated at 1.2 kW at an operating frequency of $2450\text{MHz} \pm 30\text{MHz}$. It is mounted in the head unit which also includes the filament transformer, control interlocks and feedback electronics for the power supply. Maximum power is specified for an input water temperature of 35 deg C, with a nominal lifetime, into a matched load, of 3000 hours.

The power supply provides constant anode current at a cathode voltage of -4.5kV. The filament transformer is supplied at 230V ac. The microwave power level is controlled by an analogue signal from the TCU. Alarm and trip circuits are provided, with all power and enable circuits controlled via the TCU.

2.6 Thermal Subsystem

The thermal conditions within the engine are quite different for narrow band or broadband magnetron operation. For broadband operation the majority of the input microwave power is reflected at the thrust module and dissipated in the isolator. To provide the necessary cooling, water is pumped through both the magnetron and the isolator load. For narrowband operation, the microwave power is largely dissipated in the thrust module itself. The engine layout allows for the addition of extensive radiator finning on the walls of the thrust module, if narrowband operation is used.

To support the design of the water cooling and radiating thermal sub system, a test rig was manufactured and a series of thermal tests carried out. The test rig was constructed to similar dimensions, and with the same layout, as the engine, and was capable of being mounted in the same attitudes. The coolant loop incorporated a 2kW pre-heat unit and pump together with two radiators. Mounting the pump between the two radiators ensured the pump remained primed in all three mounting attitudes.

The tests were carried out using eight thermocouples linked to a computer via data logging electronics, and enabled design verification of all the subsystem components. An inter-cooler unit was manufactured using fabrication techniques proposed for the engine. This was incorporated into the final thermal tests and confirmed the thermal radiation calculations.

The preheat unit was retained in the actual engine coolant loop to enable thermal simulation tests to be carried out during the thrust measurement programme. The unit also provides a method of pre-heating the coolant, to limit the initial temperature rise of the magnetron. A third radiator was also incorporated in the subsystem, to enable long test runs to be achieved during dynamic testing.

2.7 Telemetry and command subsystem

The design of the telemetry and command subsystem, together with power supply considerations resulted in the engine being connected to four major units. A high voltage power supply unit (HVPSU) provides the magnetron cathode and filament currents. A Telemetry and Command Unit (TCU) provides power and control commands for the magnetron, coolant pump, preheat unit and tuning drive. The TCU also interfaces and pre processes up to 8 digital and 11 analogue telemetry channels. These are used to monitor temperatures, microwave power measurements, tuner positional data and engine component status. The TCU also provides displays for temperature, tuning, and power readout.

During test runs, a Remote Command Unit (RCU) is used for control purposes and a Telemetry Computer is used to record all engine telemetry and test instrumentation data.

3.ENGINE TEST PROGRAMME

3.1 Small signal Tests

To enable sweep tests of the resonance tuning mechanism to be carried out, breadboard circuits to drive the stepper motor and to monitor tuner position and resonator power were designed and built. (These circuits were then incorporated into the TCU.)

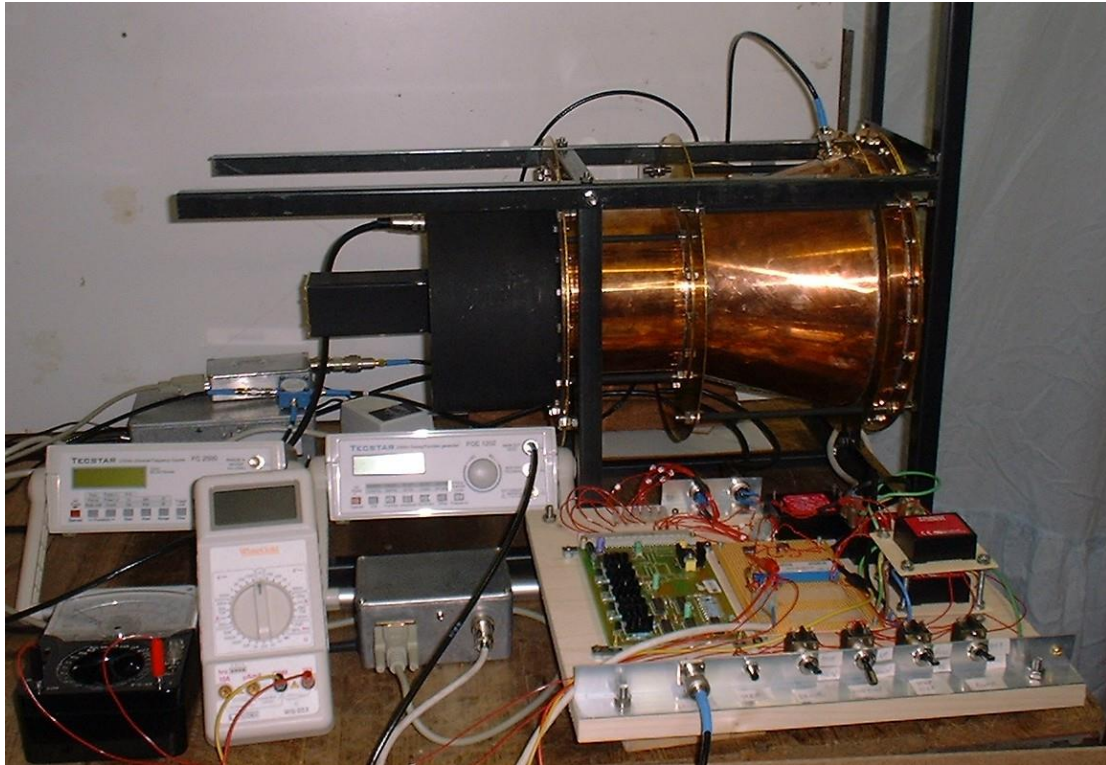
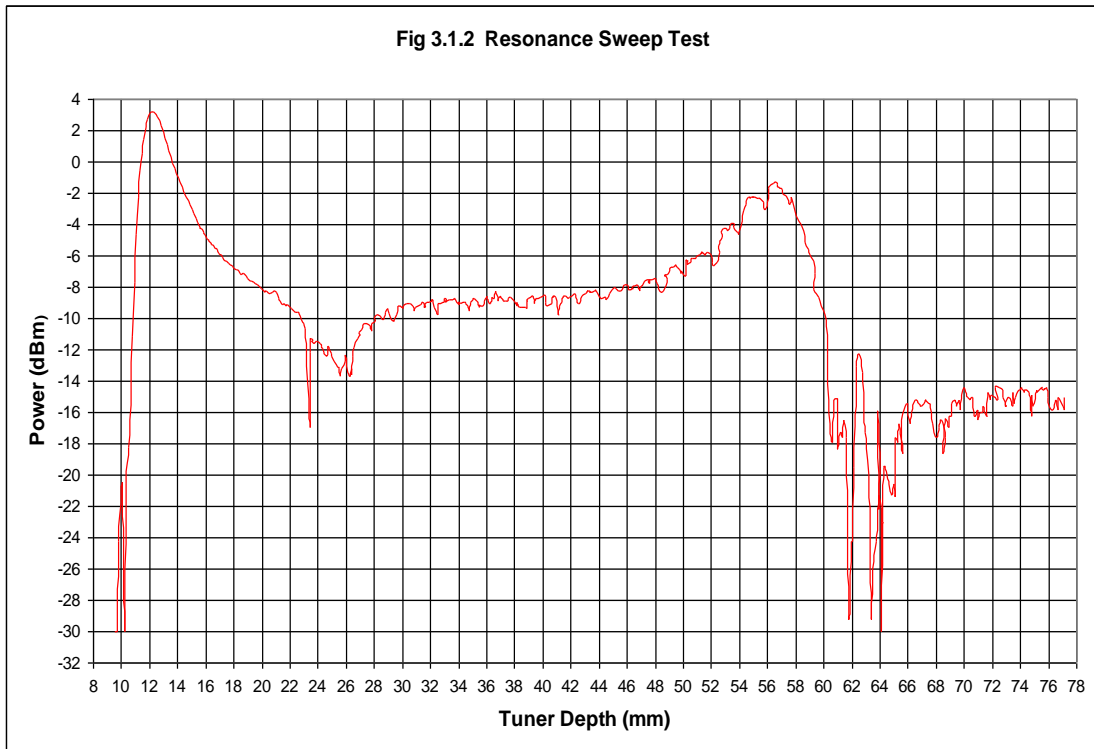


Fig 3.1.1

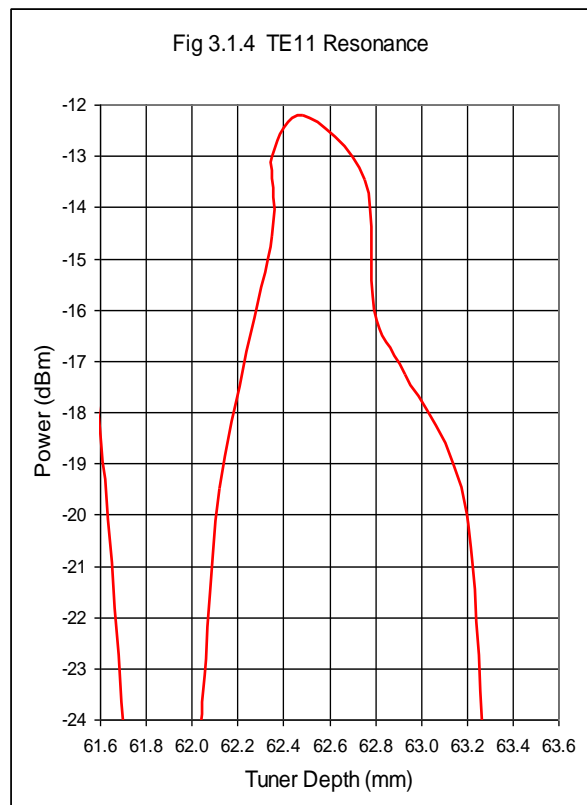
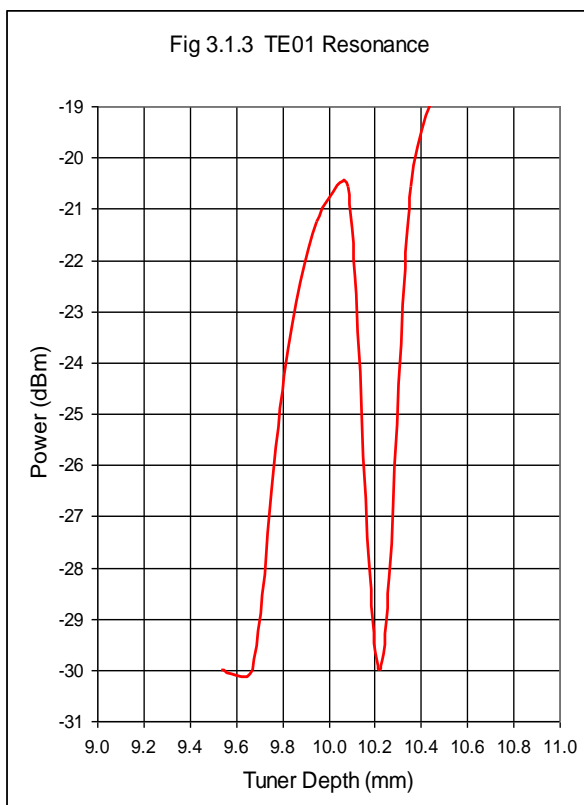
The first series of tests, illustrated in fig 3.1.1, enabled the thruster to be characterised over its full tuning range. The position of the tuning plate was stepped through its range, whilst the output from a detector probe mounted in the resonator was recorded on the telemetry computer. A crystal stabilised low power signal at a frequency of 2449.9 Mhz was fed into the input port of the resonator.

Fig 3.1.2 gives the detector output for the full tuner depth range from 8 mm to 78mm. As the input impedance was unmatched, a drop in detected signal is seen as the tuner went through resonance, with a single clear resonance peak detected for both TE01 and TE11 modes.

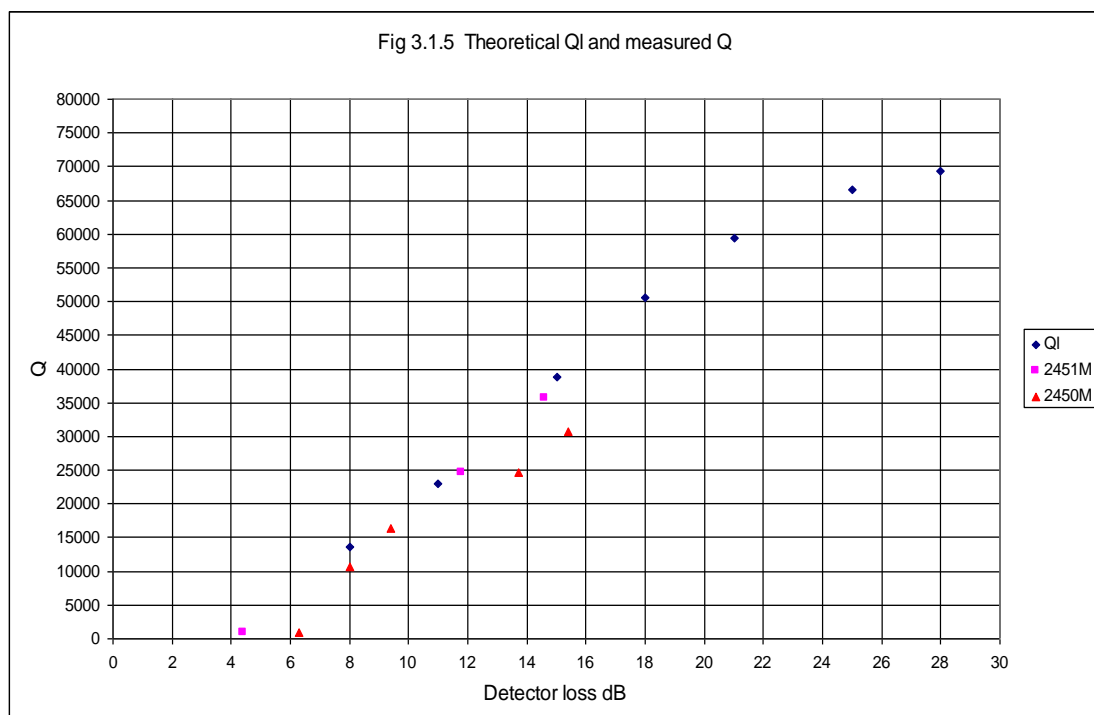
The tuner depths at which resonance was detected i.e. 10.1mm for TE01 and 64.5mm for TE11 fall within the range of theoretical depths that were obtained by running the design software for the thruster dimensions, plus and minus the manufacturing tolerances. A small resonant peak is seen around 26 mm corresponding to the TM01 mode. Running the design software for the as-built dimensions, resulted in very good agreement with the measured resonance depth, for the operational TE01mode.



Figs 3.1.3 and 3.1.4 show the two resonance peaks with Q values of 8,194 for TE01 mode and 5,257 for TE11 mode. This is in accordance with field theory, which predicts a lower surface resistance and hence higher Q for TE01 mode.

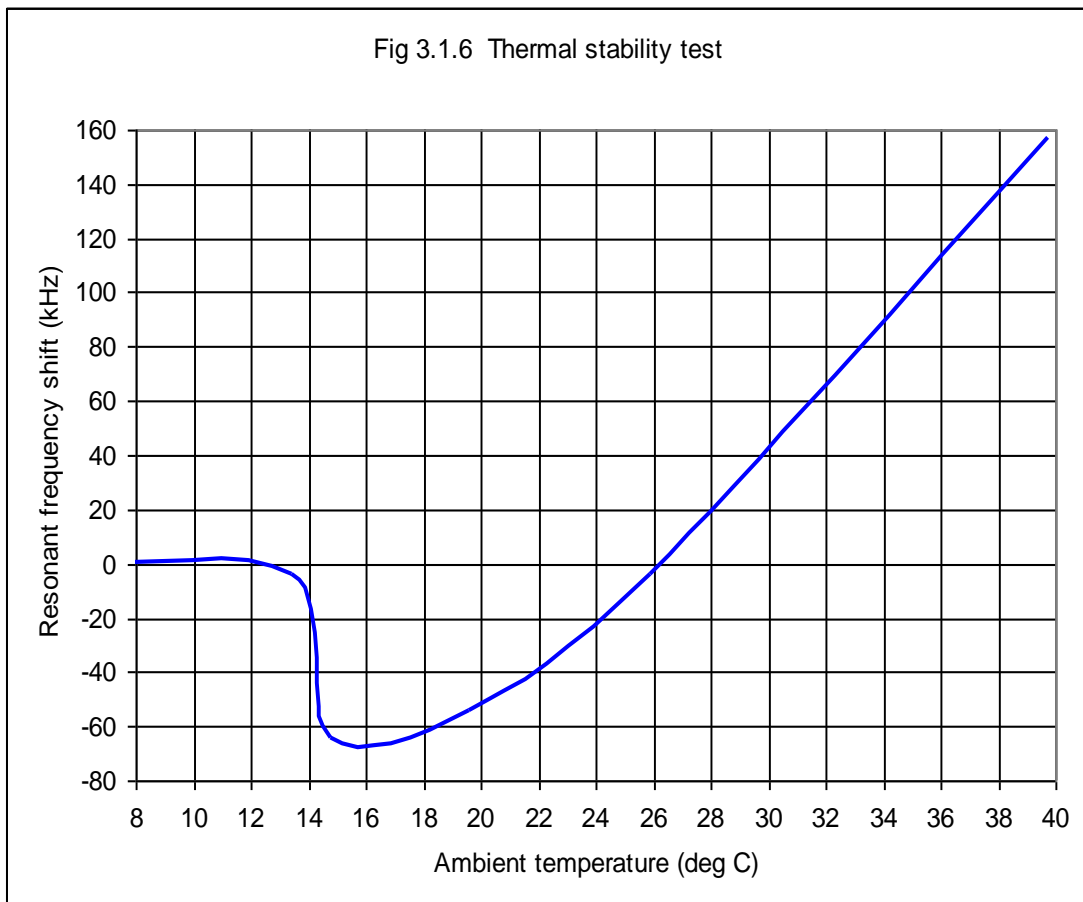


A number of detectors with decreasing sensitivity (ie increasing loss) were then used to produce a more accurate measurement of Q at the TE01 resonance position. Two different signal sources were used, one at 2449.9 MHz, the other at 2451.1 MHz .Note that any direct measurement of this very high Q value is modified by the loss introduced by the detector itself. The results are plotted, together with the theoretical loaded Q (Q_l) for increasing detector loss in fig 3.1.5. The test data points fit well with the theoretical characteristic.



A second series of tests were carried out with the thrust module enclosed in a thermal hood, enabling a 32 degree ambient temperature rise to be achieved. The results are given in fig 3.1.6 which show that the resonant frequency remains within +160kHz to -70kHz over this temperature range .This is well within the required stability.

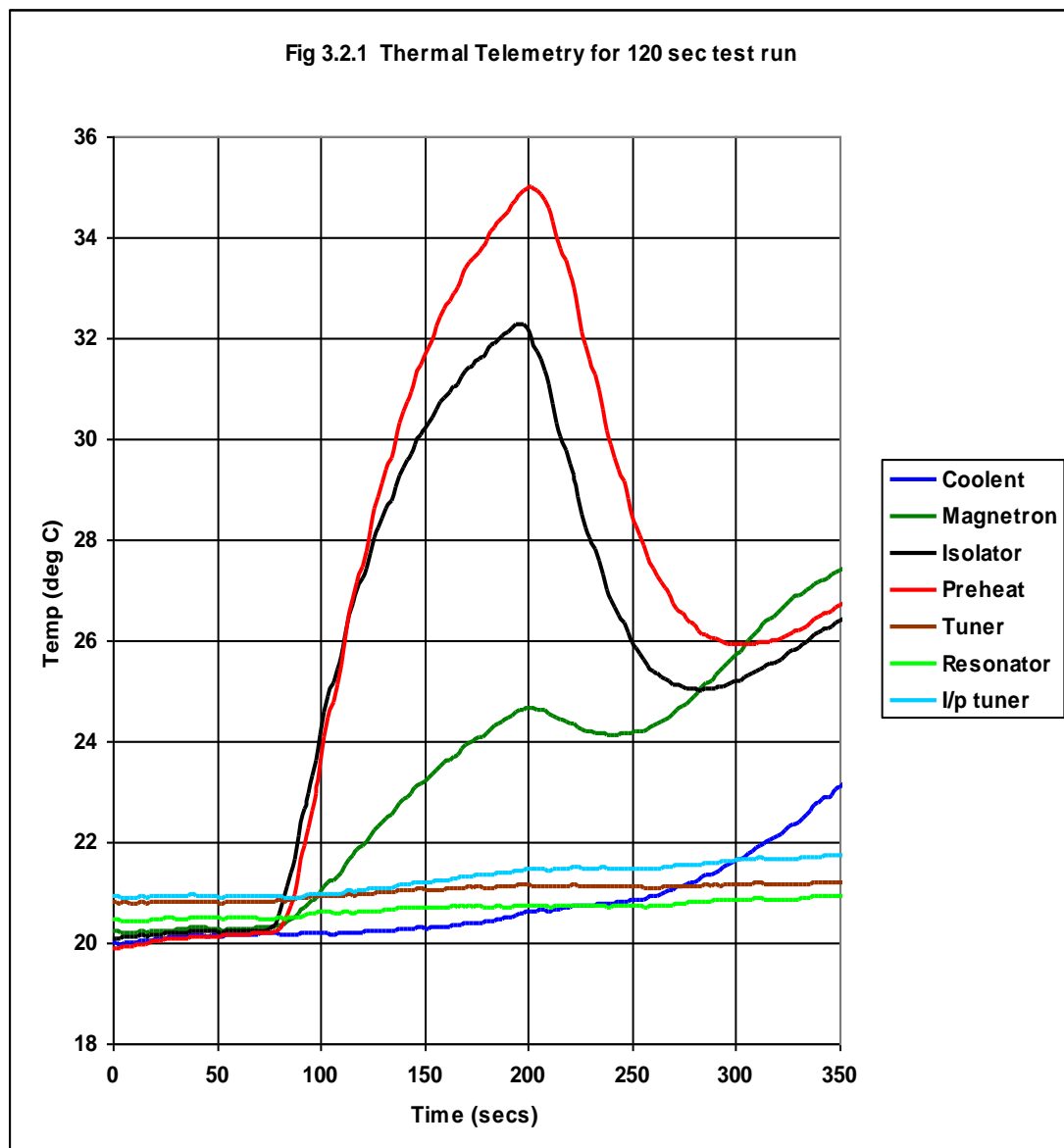
Fig 3.1.6 Thermal stability test



A total of 57 small signal sweep tests were carried out, producing a set of data which has validated the microwave and thermal compensation design process.

3.2 High Power Tests

The initial high power test runs were carried out with the input tuner settings that had been optimised from a series of low power microwave development tests. A sequence of tests were then carried out with increasing magnetron power settings, whilst the temperature telemetry was carefully monitored. The initial 2 radiator configuration allowed a number of consecutive 60 second test runs to be carried out without excessive coolant temperature rise. (Note the 60 seconds refers to the magnetron 'on' period). However, later in the vertical test programme, coolant flow problems occurred in the vertical down attitude, leading to one case of a magnetron over-temperature trip, and to the eventual failure of the preheat element. In the final 3 radiator configuration, horizontal test runs of 120 seconds duration gave coolant temperature rises of less than 0.5 degree C. Fig 3.2.1 gives a typical set of temperature data for a 120 second run where the magnetron is on between 80 and 200 seconds. During this period magnetron temperature increased 4.3 deg C, and isolator temperature increased 11.62 deg C, for a coolant temperature increase of 0.43 deg C.

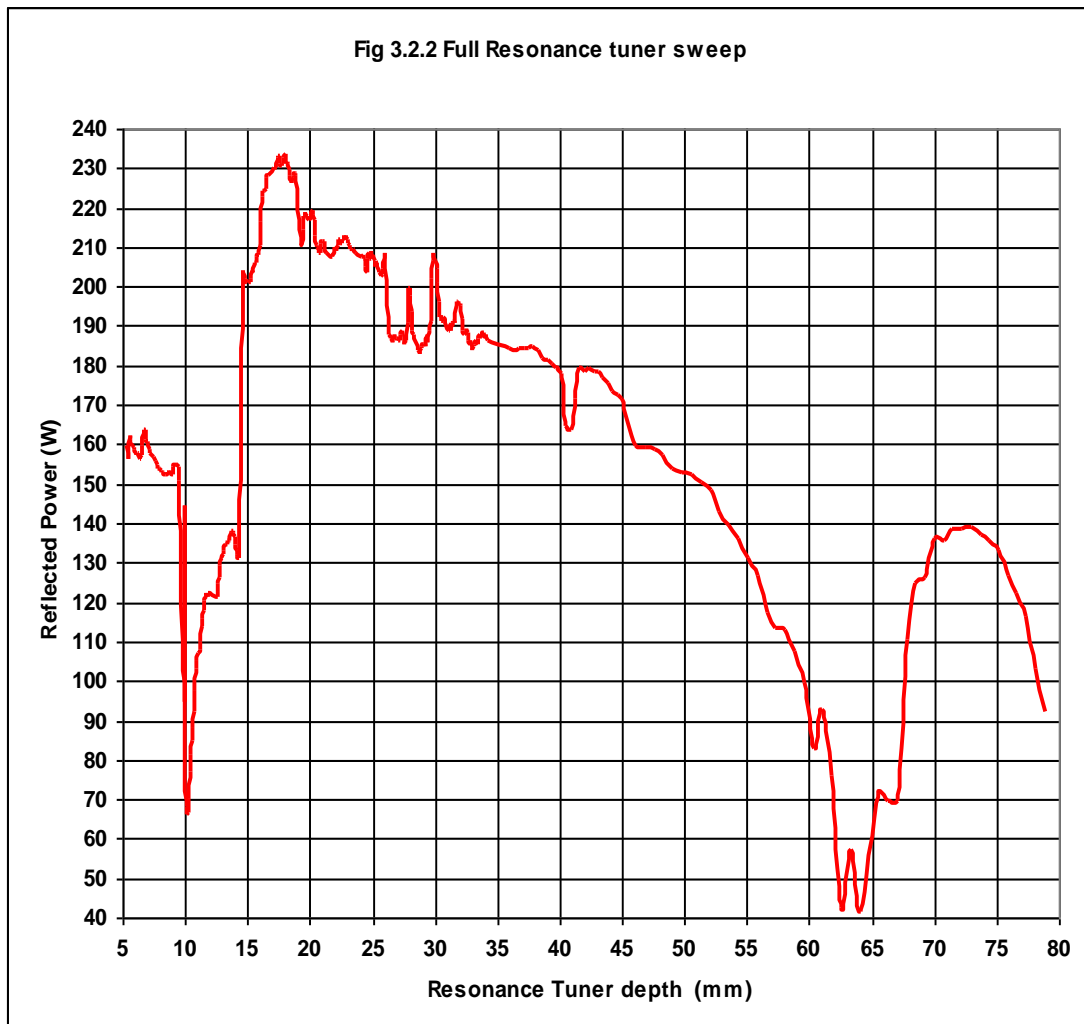


The coolant is monitored at the magnetron input and the high thermal capacity of the whole loop causes the temperature to continue to rise as the preheat, isolator, and magnetron sensors record initial cooling after switch off. Eventually, these 4 temperatures equalise during the slow cool down period.

The preheat temperature is the coolant temperature in the preheat unit and records the highest temperature reached in the loop.

The overall temp increases for Tuner section (0.35deg C), Resonator section (0.4 deg C), and Input Tuner (0.8 deg C) give an indication of the microwave loss distribution in the thruster.

With the magnetron at a mid power setting, the engine was then tested over the full resonator tuning range. Fig 3.2.2 gives a composite result of the reflected power for a number of swept tuner tests. These tests showed TE01 resonance over approximately 5MHz bandwidth, which corresponds with the quoted output bandwidth of the magnetron. A TE11 resonance mode was also measured. Both resonance points aligned closely with those obtained during the low power tests and with the theoretical design.



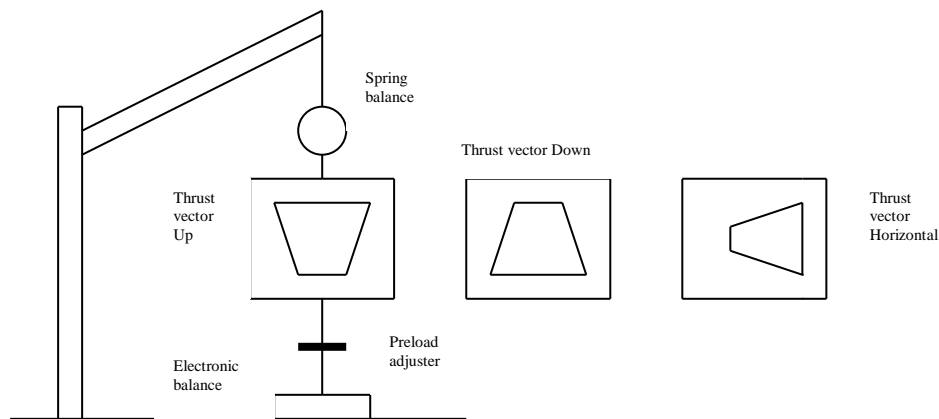
Calibration of the microwave power telemetry was carried out by first calibrating the DC circuits for a reference input voltage. The DC measurement could then be referred to the microwave input using the calibration data provided by the manufacturer of the power meter units. The input to these units from the coupler was then calibrated by connecting the coupler between the magnetron output and the circulator input. This enabled calibration using only forward power flow. The calibration was completed by connecting the coupler between the circulator output and a waveguide short circuit. This gave a final calibration for simultaneous, equal, forward and reflected power flows.

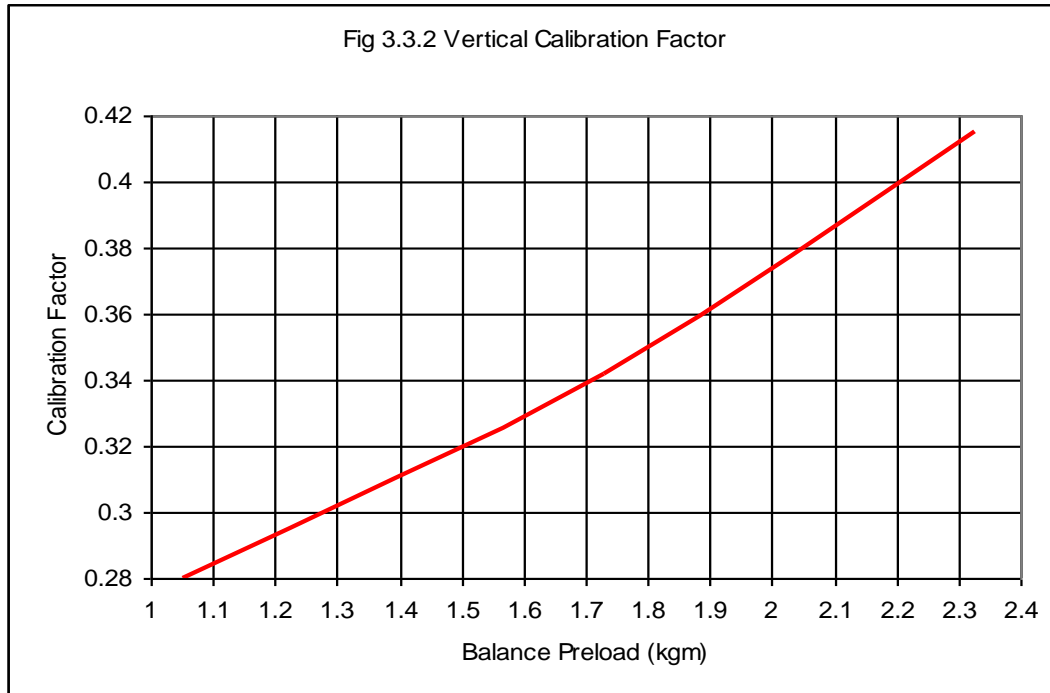
3.3 Vertical Thrust Tests

3.3.1 Description of Test Rig

The engine development tests were carried out using a direct balance technique, with the engine suspended from a crane. The majority of the 45kg weight of the engine was supported on a spring balance, with residual weight supported on the 16 kgm electronic balance, via an interface plate with a preload screw adjustment. A diagram of the test rig is given in Fig 3.3.1. The preload could be set to give an overall resolution of 0.3gm. Calibration was carried out using standard weights. The calibration characteristic is given in Fig 3.3.2. The calibration factor is the result of the two spring constants forming a composite balance. The recorded balance data is divided by the calibration factor to give the calibrated data.

Fig 3.3.1. Vertical Test Rig





The stability of the calibration was however compromised initially by changes in ambient temperature, causing minor dimensional changes in the crane and suspension. These were minimised by applying thermal lagging to the critical areas. Stability was tested using a hot air blower, with lagging applied until sufficient improvement was obtained, to enable the test runs to be carried out successfully. Minor slope corrections are applied during data processing. Thermal calibration runs were also carried out in all three engine attitudes using the preheat function. This enabled residual centre of gravity effects to be measured and compensated for, in the processing of the results.

Although the majority of the test runs were carried out with the engine thrust vector vertically up (i.e. the measured weight decreased while the engine was running), a number of runs were also carried out with the thrust vector vertically down. In these tests, the measured weight increased whilst the engine was running. Further tests were also carried out with the thrust vector horizontal, when the weight change recorded, was due only to thermal effects.

The vertical thrust test rig is illustrated in Fig 3.3.3 with the thrust vector horizontal forward.

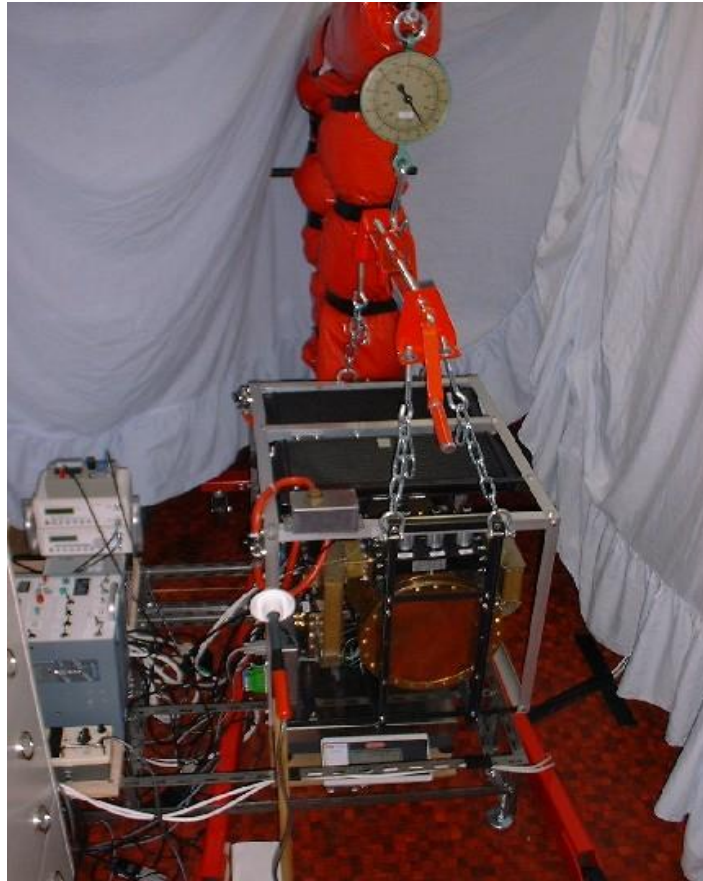
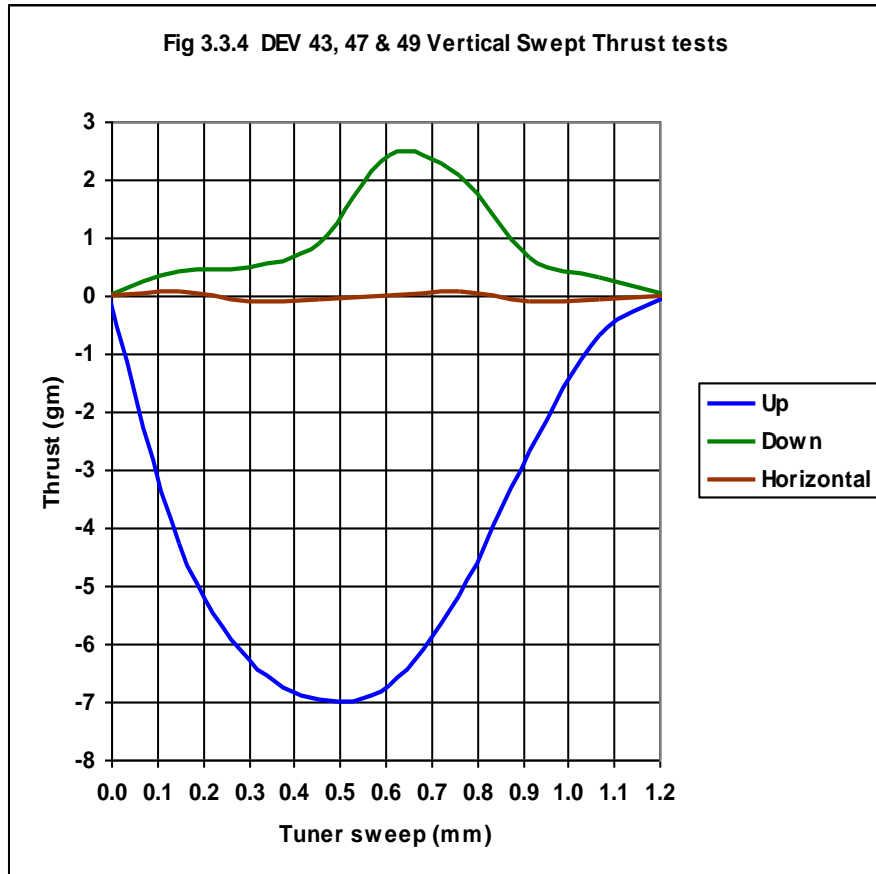


Fig 3.3.3

3.3.2 Test results

To accurately establish the optimum resonance tuner setting, a number of swept resonance tuner runs were carried out. The stepper motor driven, resonance tuner, incorporates a feedback potentiometer enabling accurate position telemetry to be recorded. The results for Up, Down and Horizontal runs are given in Fig 3.3.4.

The early test runs were carried out with non optimised input tuner settings and gave considerable variation in the thrust outputs from run to run.

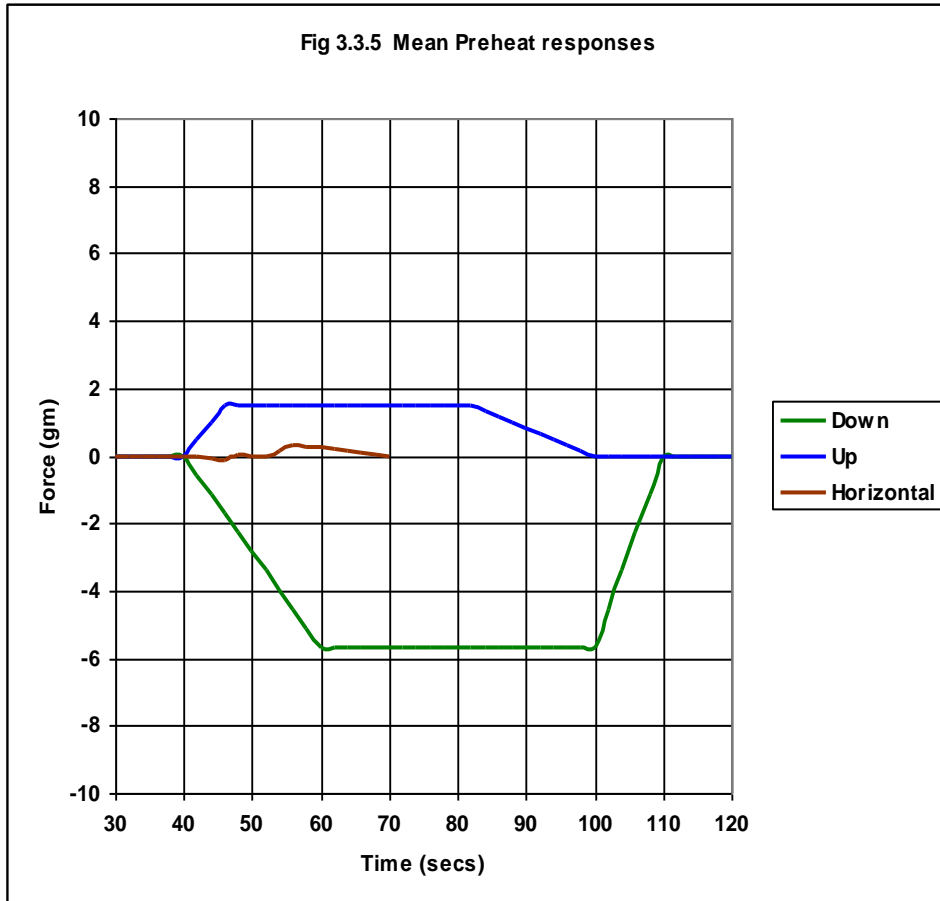


The swept tuner tests show that although the bandwidth of the magnetron output is 5 Mhz (corresponding to 5 mm) careful tuning to within 0.1mm is required, to select the max component within the available output spectrum.

A series of thrust measurement test runs were then carried out using a sequence of different input tuner settings. The input tuner stubs were manually set using multi-turn precision indicators on each stub. In this manner, the input match at the high power magnetron setting was gradually improved, to give increased levels of thrust, with higher input powers to the engine. From an initial thrust of 1.28 gm at 193 Watts, thrust was increased to 8.33 gm at 744 Watts. The sequence of tests is given in Table 3.3.1.

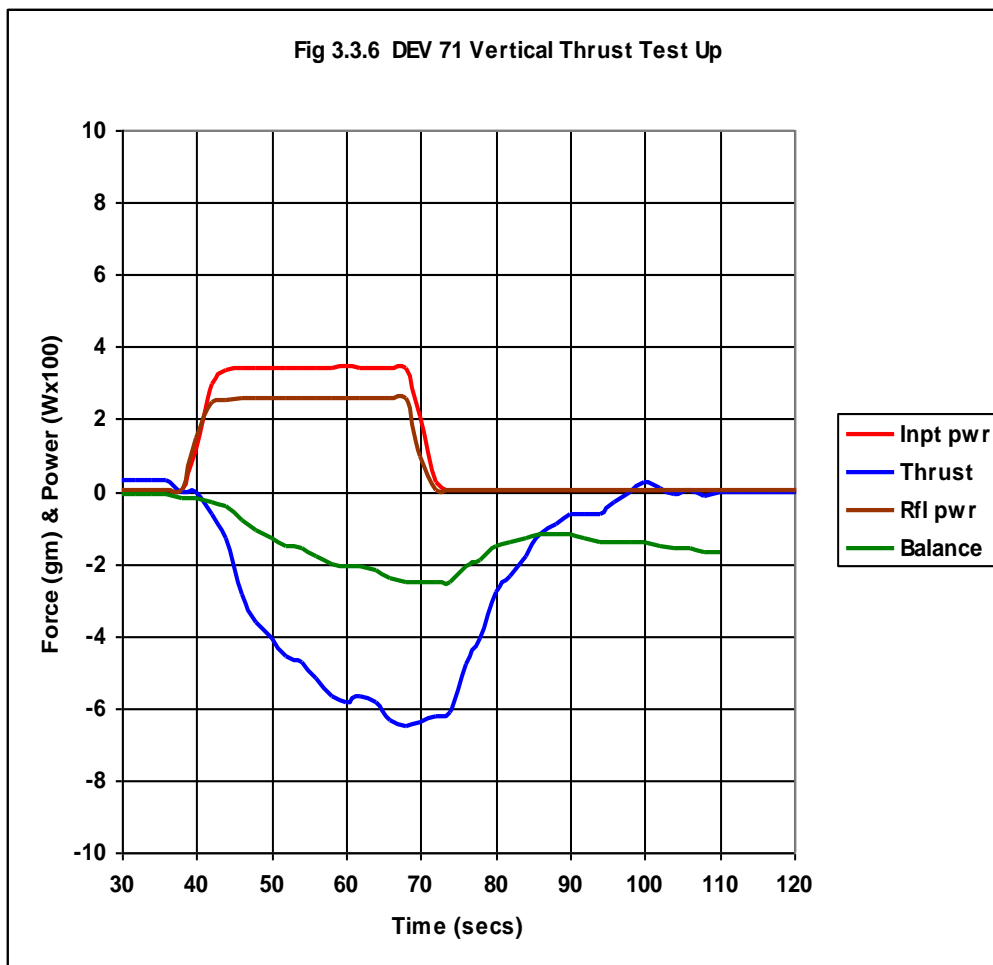
The thrust data given is the mean of the processed telemetry data. The processing removes any test rig response slope. A typical slope can be seen in the 'Balance' plot in fig 3.3.6. The data is then divided by the calibration factor, which varies with the preload on the balance and is given in fig 3.3.2. Finally the mean preheat response is subtracted, which, from fig 3.3.5, can be seen to be the major correction factor. The mean preheat responses for Up and Down and Horizontal configurations are given in fig 3.3.5. Comparison between the raw balance data and the thrust data in fig 3.3.6 shows the effect of processing.

A total of 95 vertical thrust test runs were carried out, most of them with the engine running for periods of 60 secs. Many of the test runs were carried out without the engine suspended, to enable adjustment of the input tuner stubs whilst monitoring input and reflected power.



Test ref	Thrust vector	Input tuner settings			Output power (Watts)	Mean thrust (gm)	Specific thrust (mN/kW)	Q
		S1	S2	S3				
DEV 60	Up	874	394	0	193	1.28	65	11,563
DEV 62	Up	630	0	0	404	3.73	91	16,097
DEV 65	Up	524	28	472	386	1.79	45	8,085
DEV 71	Up	630	1400	802	338	6.12	178	31,569
DEV 74	Up	918	1400	584	552	4.18	74	13,203
DEV 77	Up	630	1400	584	561	4.05	71	12,587
DEV 78	Up	778	1400	584	543	4.34	78	13,935
DEV 81	Up	848	1400	584	572	3.4	58	10,363
DEV 82	Up	778	1400	693	443	3.8	84	14,956
DEV 83	Up	778	1400	471	697	3.94	55	9,856
DEV 84	Up	778	1400	358	914	4.12	44	7,859
DEV 85	Up	630	1400	358	887	4.31	48	8,472
DEV 88	Down	630	1400	358	820	5.54	66	11,779
DEV 89	Down	630	1400	358	744	8.33	110	19,521
DEV 91	Down	778	1400	584	534	4.62	85	15,084
DEV 92	Down	778	1400	584	512	5.05	97	17,197
DEV 94	Horizontal	778	1400	584	530	0.19		
DEV 95	Horizontal	778	1400	584	516	0.37		

Table 3.3.1 Vertical Thrust Tests



The results of test run DEV 71 are illustrated in Fig 3.3.6. This run recorded the highest specific thrust of 178mN/kW, giving a calculated Q of 31,569. The high Q results from the low loading effect of the input tuner setting. This also gives a high ratio of reflected power compared to input power. The magnetron was on for a period of 30 secs in this test run.

The effect of the magnetron warm-up frequency shift can be seen in this run. The thrust builds up throughout the 30secs, as the frequency of the major component of the magnetron output is pulled into tune with the resonator. Separate frequency measurement test runs have shown different warm-up shifts for different magnetrons, and for different input tuner settings. All thrust measurement runs have shown the effect of some degree of warm-up frequency shift.

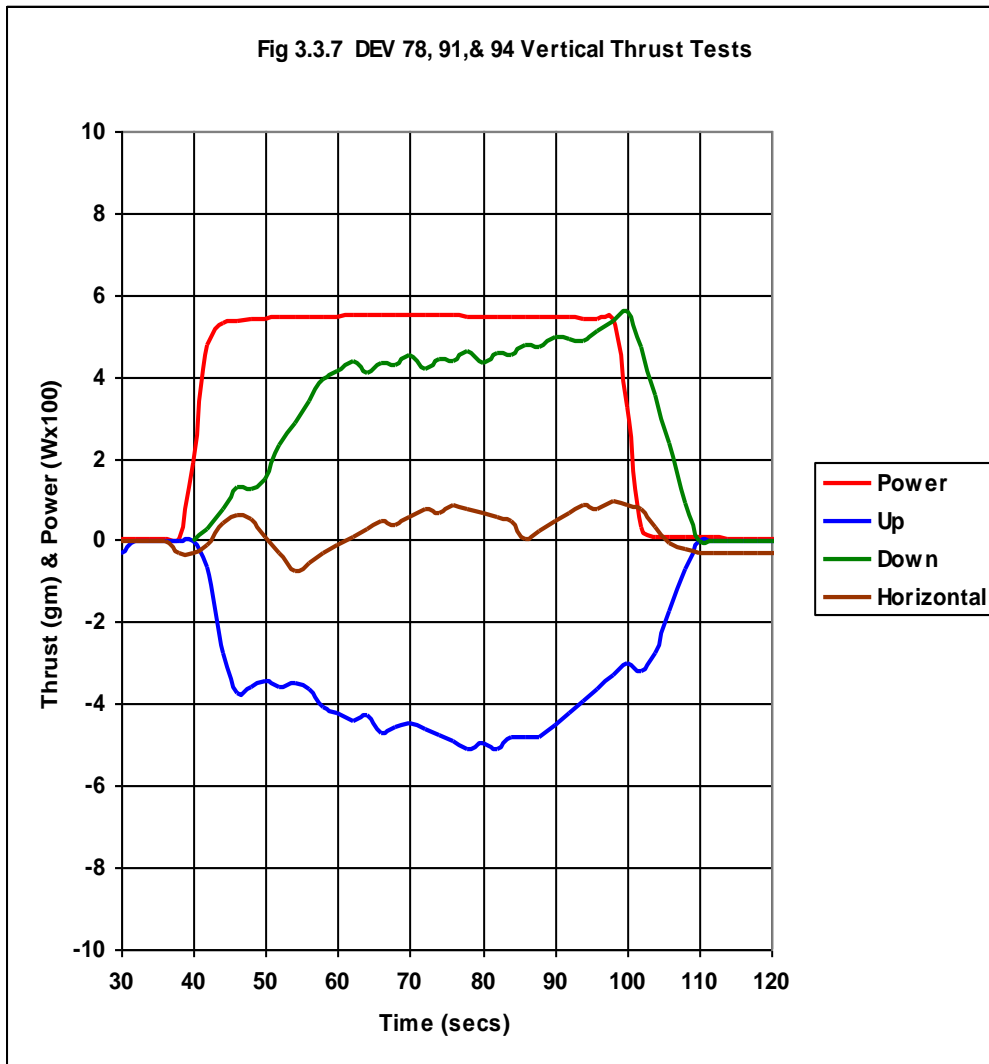


Fig 3.3.7 gives the test results for 3 test runs with the same input tuner settings, but for thrust vector directions Up, Down and Horizontal. This clearly illustrates the loss of measured weight for the Up vector, the increase in measured weight for the Down vector, and the zero mean weight change for the horizontal vector. Calculated Q values were 13,935 for the Up test and 15,084 for the Down test. As no thrust was recorded for the Horizontal test, the Q could not be calculated for this run.

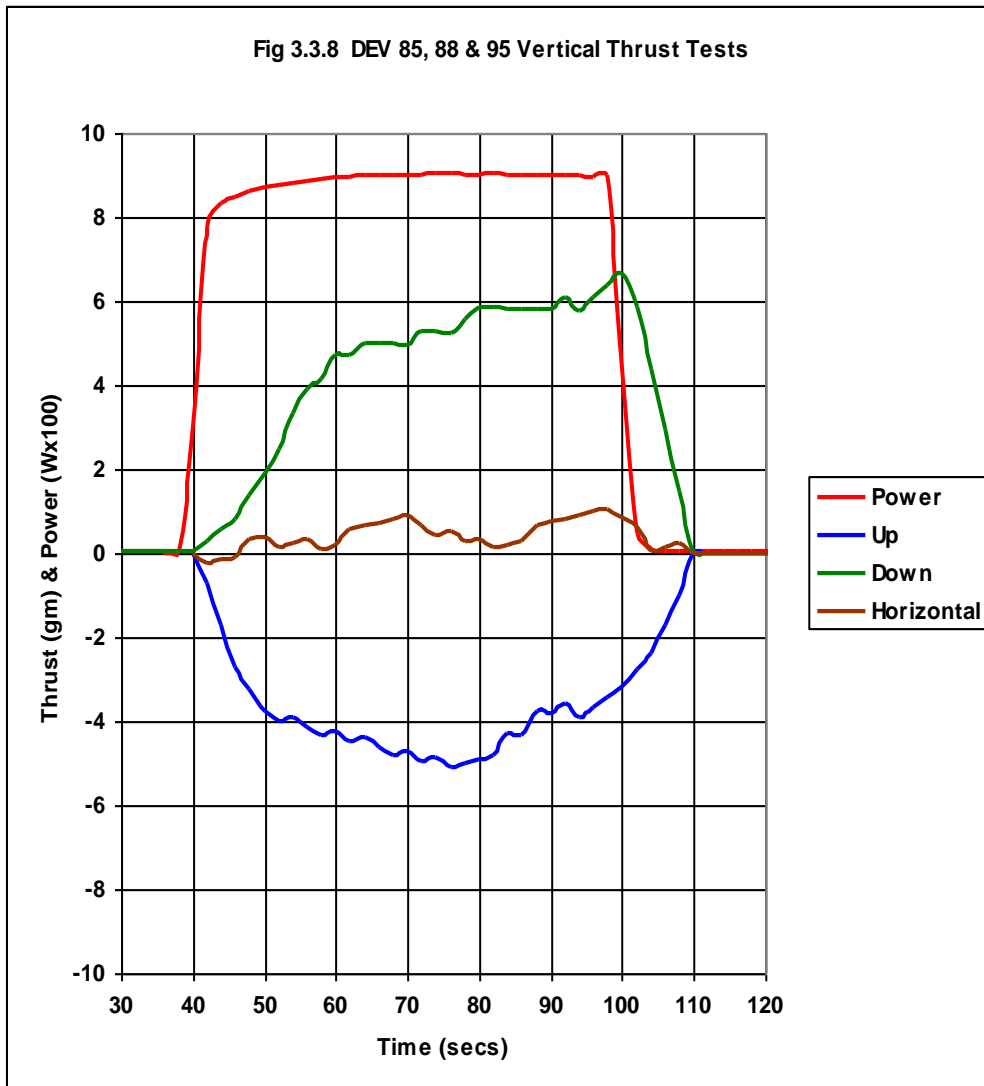


Fig 3.3.8 gives the results for Up and Down runs at the highest input powers obtained. They resulted in similar thrust values to those in Fig 3.3.7, but the higher loading of the input tuner settings, resulted in the lower Q values of 8,472 for the Up test and 11,779 for the Down test. These two sets of results demonstrate the sensitivity of the impedance match between the magnetron and the resonator.

Note that in all the vertical test runs, there is a time lag between the power characteristic and the thrust characteristic, due to the inertia of the engine, moving against the composite spring constant of the balances.

3.4 Horizontal thrust tests

3.4.1 Description of Test Rig

Following the vertical thrust tests, the test rig was then modified to enable thrust to be measured horizontally. In this configuration, the engine was suspended from the crane and a 90 degree thrust transfer rig used to transfer the horizontal thrust into a vertical force, which was measured directly using the 110gm electronic balance. Calibration was carried out by attaching a cord at the centreline of thrust and running it over a pulley to a weight pan. The rig was then calibrated using standard balance weights. A diagram of the test rig is given in Fig 3.4.1.

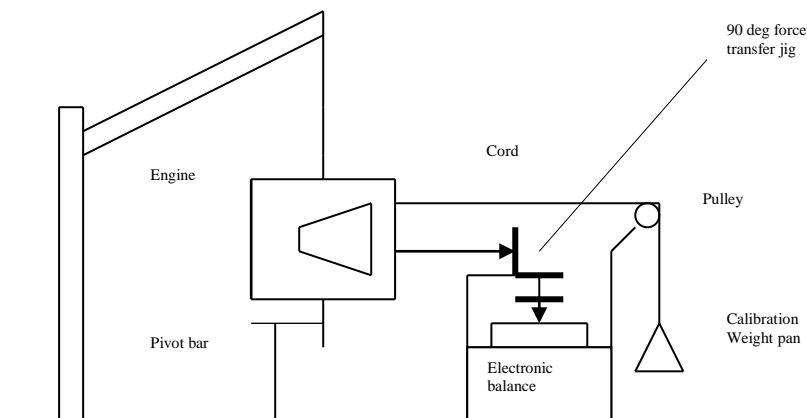


Fig 3.4.1

Calibration was complicated by the centre of gravity of the engine not being on the centre line of thrust. This caused a rotational torque to be set up and the actual thrust measured was a component of the thrust produced. To prevent the balance reaction causing Centre of Gravity movement, a pivot bar was mounted under the Centre of Gravity of the engine. The value of the measured component of thrust was calculated from the geometry of the rig, as shown in Fig 3.4.2.

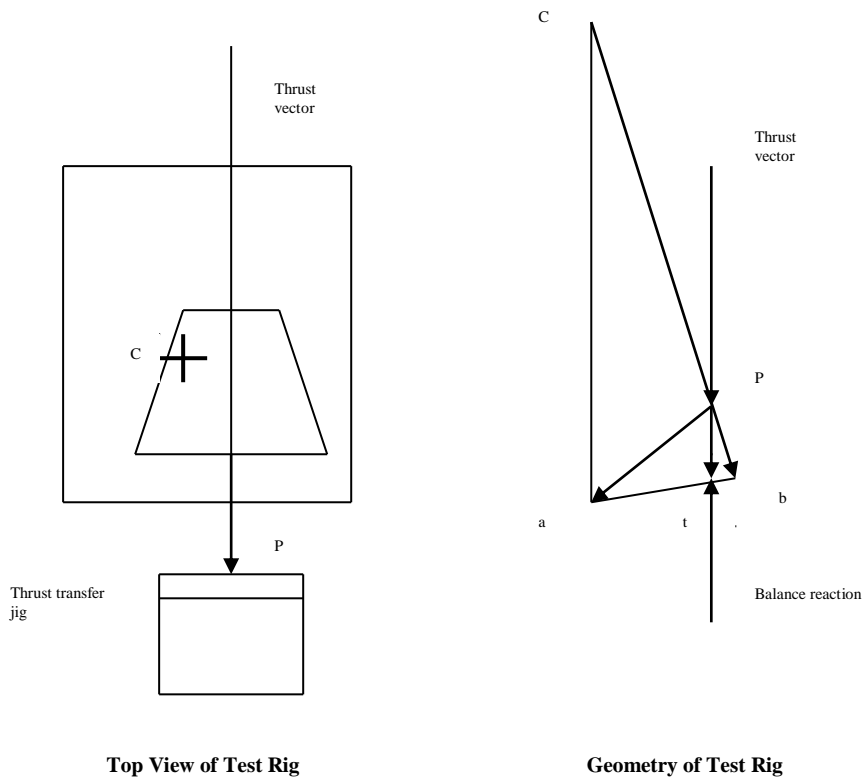


Fig 3.4.2

The thrust acting on the transfer jig at point P results in the torque around point C. It can be resolved into two orthogonal components, a and b. The force measured by the electronic balance via the transfer jig is the component t. The resulting calibration factor of .074, calculated from the as-built engine dimensions, was checked against the thrust for a similar test run with the vertical test rig. (i.e. comparison of DEV 91 and DEV 107 gives 4.62 gm for 534W input power, compared to 4.29 gm for 498 W). This gives exactly the same specific thrust for both tests. The direct use of a high resolution balance also gave a fast measurement response, enabling good correlation to be seen between thrust and input power characteristics. The test rig is illustrated in fig.3.4.3.

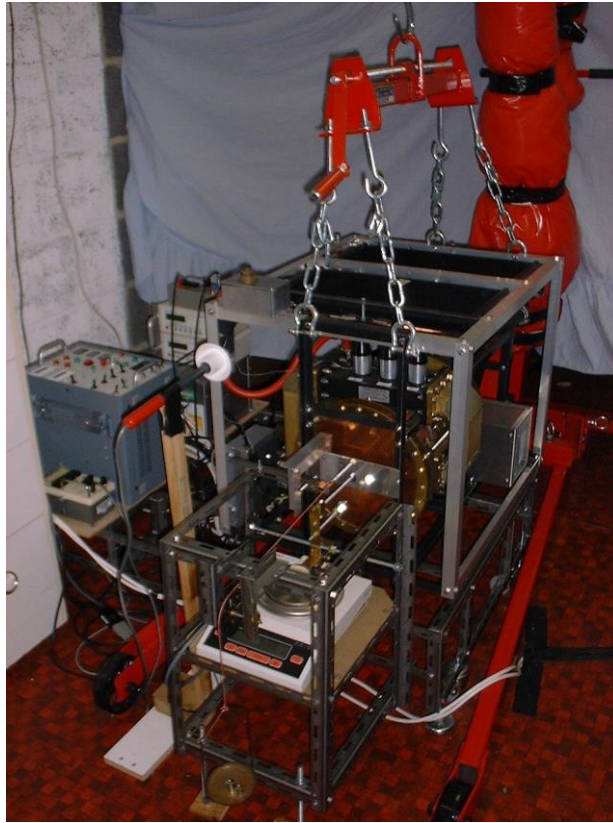
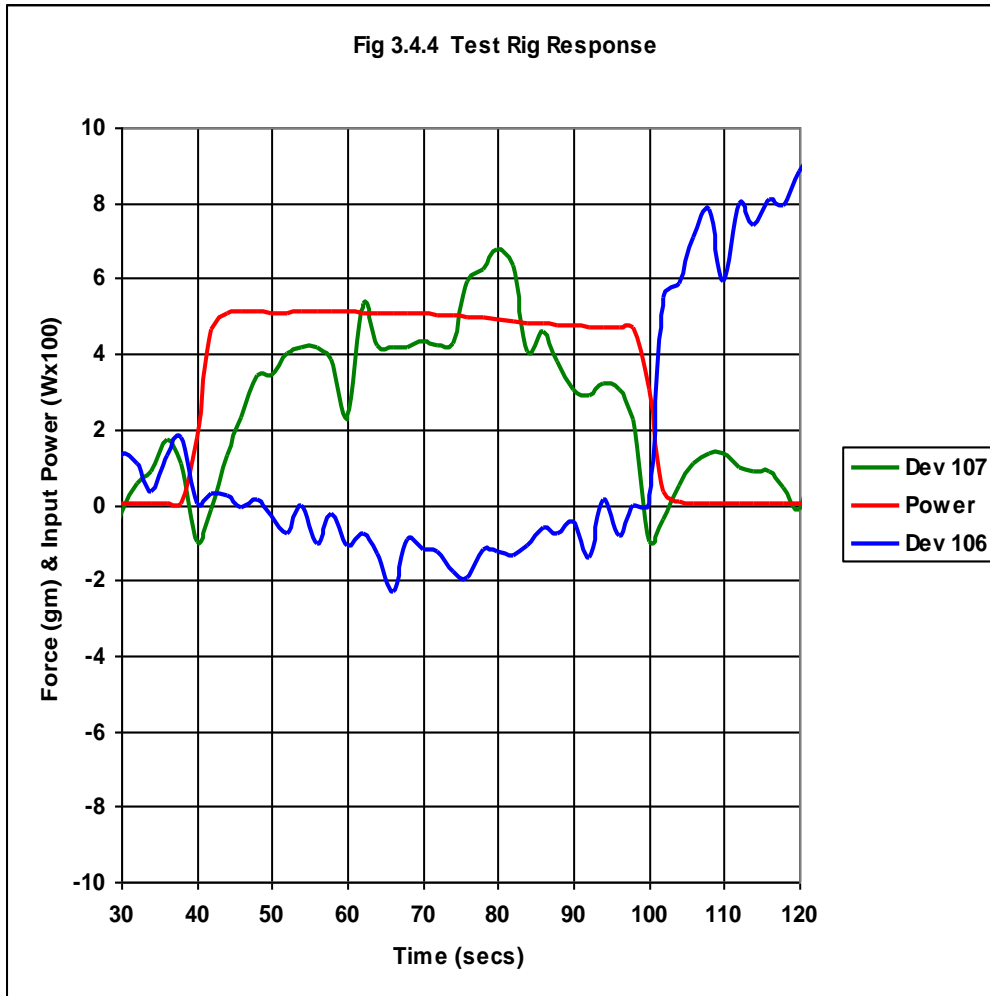


Fig 3.4.3

3.4.2 Test Results

Fig 3.4.4 shows the test rig response without the pivot bar, in test DEV 106. Without a point of reaction at the centre of gravity of the engine, no torque can result, and therefore no thrust is measured. However with the pivot bar in place, as in DEV 107 the thrust can be measured.



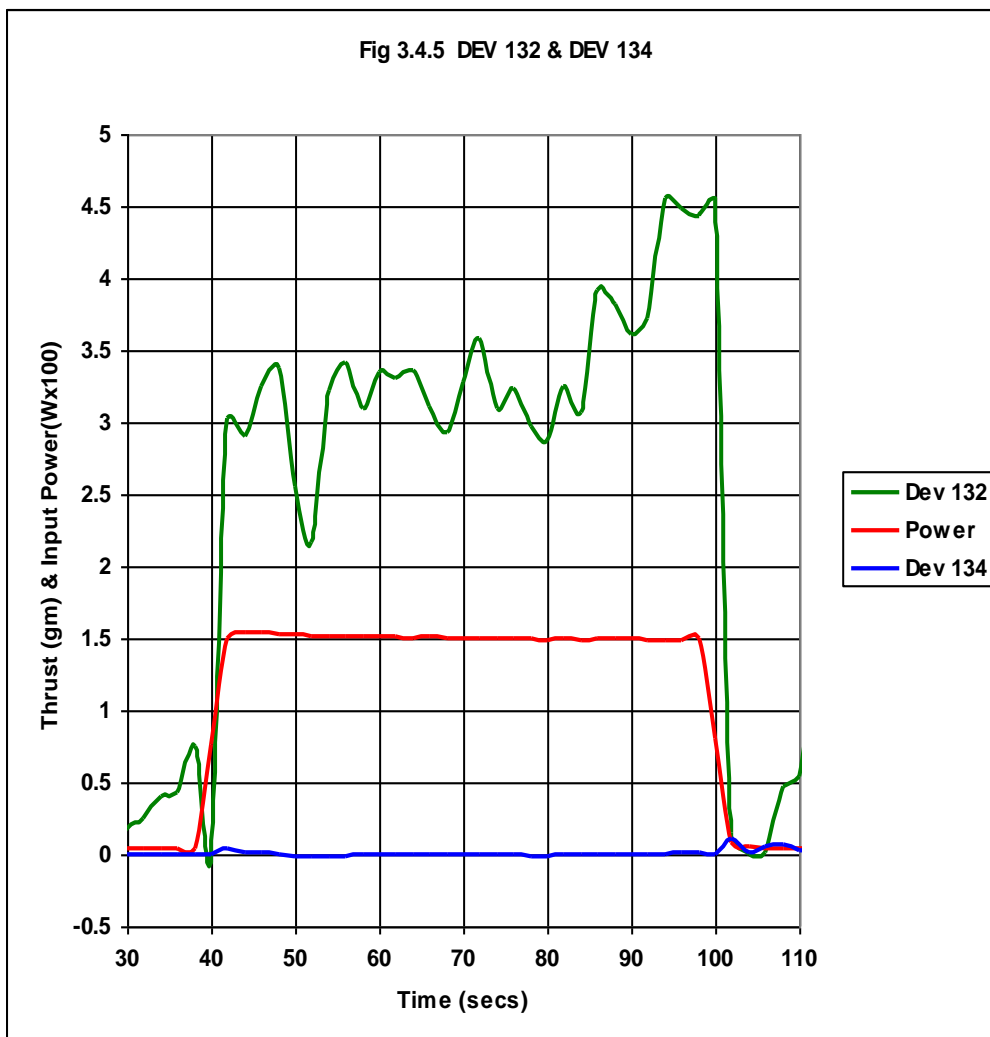
The next series of tests continued the input tuning sequence, with the results summarised in table 3.4.1. The object of the sequence was to further investigate the envelope of impedance match between tuner and resonator and between tuner and magnetron. With the magnetron power supply set to constant power settings, the results of the test runs varied from a maximum thrust of 4.87 gm for 498W input power, to 3.29 gm for 151W input power. These values correspond to Q values of 17,050 and 37,988 respectively. They illustrate the increase in specific thrust that can be achieved with a low input loading on the resonator.

Test ref DEV	Input tuner settings			Resonance tuner (mm)	Input power (Watts)	Mean thrust (gm)	Specific thrust (mN/kW)	Q
	S1	S2	S3					
106	778	1400	584	15.5	503	-0.95		
107	778	1400	584	15.5	498	4.29	85	15,019
120	778	1400	584	15.2	498	4.87	96	17,050
126	780	1400	70	15.2	357	4.87	134	23,784
130	468	1400	70	15.2	302	2.85	93	16,454
132	468	0	70	15.2	151	3.29	214	37,988

Table 3.4.1.

Note also the increase in Q, from 15,019 in DEV 107, to 17,050 in DEV 120, when the resonant tuner depth is decreased by 0.3 mm. This illustrates the need to track any frequency drift of the main spectral component of the magnetron output. Over the range of tests quoted in this report, a drift of approximately 4MHz, from 2,451 MHz to 2,447 MHz, was measured. This required a resonance tuner depth increase from 11.4 mm to 15.2 mm to maintain optimum resonance setting.

Fig 3.4.5 shows the results for DEV 132, illustrating the highest Q achieved (37,988). Also shown is DEV 134, where the test is repeated with the balance locked. This test confirms that EMC effects on the balance data are negligible.



4. Summary and Conclusions

- a) The microwave design was based on updated software used in the design of the experimental thrusters.
- b) The microwave design was validated by a series of small signal sweep tests.
- c) The thermal compensation design was validated by thermal testing of the engine under small signal conditions.
- d) The thermal subsystem design was initially tested on a thermal test rig, and was then shown to provide sufficient cooling to enable high power tests to be carried out.
- e) High power sweep tests showed good agreement with the small signal sweep tests.
- f) Vertical test rig development resulted in a fully calibrated rig capable of measuring engine thrust to a resolution of 0.3 gm.
- g) Vertical sweep tests confirmed that thrust peaked at the design resonance point.
- h) Thrust peaks were measured in the correct direction with the engine in both up and down configurations. No vertical thrust was measured with the engine horizontal.
- i) A series of vertical thrust tests with a fixed resonance setting, but with different input tuner settings, gave an envelope of performance covered by:
 - Min. 1.28 gm thrust for 193 Watts input power.
 - Max. 8.33 gm thrust for 744 Watts input power.
- j) The vertical thrust tests included up, down and horizontal engine configurations. In each case, the thrust was measured in the correct direction, with no vertical thrust being measured with the engine horizontal.
- k) A horizontal test rig was developed which enabled calibrated thrust measurements to be made with the engine in a horizontal position.
- l) The input tuning tests were continued on the horizontal test rig and gave a maximum specific thrust result of 214 mN / kW. The measured results were:
 - 3.29 gm thrust for 151 Watts input power
- m) It is concluded that the Demonstrator Engine has provided further evidence to validate the theory, and has enabled significant progress to be made towards a flight engine design.

5. Further work

In the later stages of the project, a dynamic test rig was built, based on a large rotary air bearing. It is planned that this rig will be used for acceleration tests on both the Demonstrator Engine and a new experimental superconducting thruster. The mathematical theory, given in REF 2, indicates that the Q loading effect at the very high Q value, of a superconducting thruster, will be measurable.

At present, the total weight of the Demonstrator Engine, power supplies and instrumentation is approximately 100 Kgm. To obtain consistent acceleration measurements over 360 degrees rotation, the friction torque of the bearing should result in a force that is less than one tenth of the thrust produced by the engine. With a present maximum thrust of 8 gm, this is a friction force of less than 0.8 gm. The requirement for a bearing friction force that is 125,000 times less than the load it is carrying, is presently not being achieved.

Further development work on the dynamic test rig will include a new air compressor and improved dynamic balancing.

A programme of work will also be carried out to develop a new input feed assembly. The object is to improve the magnetron to resonator impedance match, and increase the input power to the engine, whilst maintaining the optimum Q loading. This will increase the output thrust. The work will be possible following the procurement of new microwave instrumentation, including a precision sweep generator. Narrow band operation will also be investigated, using a TWTA as the microwave power source.

A combination of dynamic rig development, and increased thrust from the new input feed assembly, will enable acceleration tests to be carried out on the Demonstrator Engine.

The design of the experimental superconducting thruster has already been started. High temperature, superconducting, thin film, technology will be used in a liquid nitrogen cooled thruster. Although input microwave power levels will be low, the very high Q values lead to predicted thrust levels, which will be measurable on the dynamic test rig.

A flight design programme has also been started, to support the ongoing marketing work. This design, based on a low power C Band thruster, will make possible a technology demonstration flight within a 2 year timescale. The thruster itself will be easily mechanically qualified, and be powered by off-the-shelf, flight qualified TWTA's. Closed loop tuning will be employed, using a flight qualified synthesised signal source.